



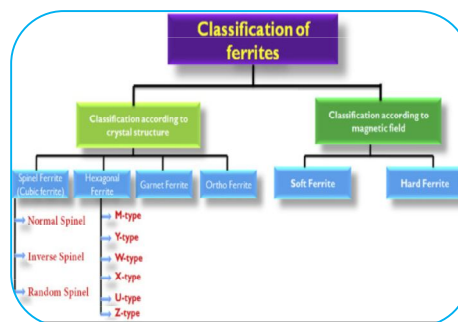
ELECTRICAL AND MAGNETIC PROPERTIES OF FERRITE

Dr. Urmi Joshi

Government Polytechnic, Jamnagar.

ABSTRACT:

As of late, ferrite nanoparticles have been widely concentrated by analysts due to their wonderful electrical properties. In the current examination, ferrite nanoparticles were ready by co-precipitation technique utilizing ferric chloride $FeCl_3 \cdot 6H_2O$ and $ZnCl_2/BaCl_2$ as natural substances. The response was done in antacid mode of sodium hydroxide arrangement. The nanoparticles incorporated and strengthened at $400^\circ C$. The incorporated ferrite nanoparticles were described by X-beam diffraction (XRD), Fourier change infrared (FTIR) spectroscopy and Thermogravimetric Differential filtering calorimetry (TG-DSC). The morphology was concentrated on utilizing SEM and observed that morphology is better for charge transportation in ferrites. The hysteresis M-H circles for this examples was determined utilizing Vibrating Test Magnetometer (VSM). The Electronic impedance spectroscopy (EIS) shows the electrical reaction of the ferrite nanoparticles in a large number of frequencies (1 kHz to 1MHz) at room temperature.



KEYWORDS: Ferrite nanoparticles, co-precipitation, hysteresis, morphology.

INTRODUCTION

Attractive nanoparticles in light of their exceptional physical and substance properties certainly stand out in different fields from innovation to biomedical applications [1]. The most intriguing and testing issues of the study of attractive nanoparticles is the presentation of new electronic, optical or photochemical properties and the improvement of their attractive properties [2]. The interest in research connected with metal spinal ferrite nanoparticles has expanded altogether as of late because of their possible applications in ferrifluides, magnetoptics, spintronics, biomedical applications and anodes for batteries [3-7]. Because of their remarkable size and shape, they can without much of a stretch reach to the body parts where other regular medications view as difficult to reach. The size of the particles relies for the most part upon the planning technique and conditions [8,9].

Among different attractive nanoparticles, spinel $ZnFe_2O_4$ and $BaFe_2O_4$ nanoparticles are broadly concentrated because of their capacity to shape an ideal attractive framework toward understanding and controlling attractive properties at the nuclear level through compound control [10]. Zinc ferrite is a genuine illustration of the immediate connection between the nanoparticle design, organization and properties [11-14]. At the point when ready as a mass material, the zinc-iron oxide has a spinel structure AB_2O_4 with a tetrahedral A site involved by Zn^{2+} particles and an octahedral B

site by Fe³⁺ particles. Similarly, Barium ferrite is a notable [15,16], elite execution, extremely durable magnet material with an enormous magnetocrystalline anisotropy along its hexagonal design and a somewhat huge magnetisation, as well as an incredible compound dependability and consumption resistivity [17]. Many sorts of creation strategies have been accounted for getting ready spinel ferrite nanoparticles for these reasons, e.g., sol-gel techniques, the ball-processing procedure, co-precipitation, electrospinning strategy, the aqueous technique, the opposite micelles process and the miniature emulsion technique [18-22]. Ammar et al., arranged zinc ferrite nanoparticles by constrained hydrolysis in a polyol medium. They announced that the magnetisation was expanded with diminishing the size of the zinc ferrite nanoparticles. Yang et al., integrated zinc ferrite nanoparticles by the tartrate antecedent technique. Drofenik et al., integrated zinc ferrite nanoparticles by utilizing ultrasonic radiation. Bardhan et al., integrated zinc ferrite nanoparticles by strong state ignition technique. Swamy et al., arranged zinc ferrite nanoparticles by self-proliferating low-temperature ignition technique [23-27]. To defeat the above strategies co-precipitation strategy has been seriously examined to incorporate the forerunner [28]. For model, spinel ZnFe₂O₄ and BaFe₂O₄ was integrated by this strategy, which incredibly decrease the creation cost.

Here, we report on a lot less complex and economical strategy, for planning spinel ferrites. The item was strengthened and described by powder XRD, FT-IR spectroscopy, Filtering electron microscopy and DSC investigation and the attractive property was portrayed by vibrating test magnetometer (VSM). The dielectric steady and conductivity reads up likewise detailed for the spinel ferrites.

Throughout recent years specialists have been engaged with blend of Li doped cobalt ferrites with demonstrated improvement in electrical and attractive properties like expansion in resistivity and coercivity with moderate immersion charge.

EXPERIMENTAL METHODS

Materials

Iron chloride, Zinc chloride, Barium chloride and sodium hydroxide purchased from Merck, were of purity 98-99%. The chemicals were used as such without further purification.

Experimental procedure

Zinc ferrite and Barium ferrite nanoparticles were prepared by co-precipitation method [29], using starting material of iron chloride hexahydrate, FeCl₃·6H₂O and Zinc chloride. 25 ml of zinc chloride, ZnCl₂ solution were mixed with 25 ml of iron chloride solution in 250 ml beaker. The solution was constantly stirred with the help of magnetic stirrer. 25 ml of 1.5 M solution of NaOH was added drop wise to adjust the pH of solution 11-12, with constant stirring. The reaction is carried out in higher values of pH, because in this pH range the size of the particles as well as their nucleation rate is controlled, as reported in Jolivet, J.P., et al., 1997. The solution was then brought to reaction temperature of 80°C. The solution was stirred for 60 minutes and subsequently cooled to room temperature. The solution was decanted and washed twice with distilled water and finally with ethanol to remove the impurities and excess surfactant. The synthesized nanoparticles were centrifuged for 15 minutes at 3500 rpm and dried overnight at 100°C. The powder nanoparticles were used for further characterisation studies. Barium ferrite nanoparticles were also prepared by the above procedure.

Characterisation

The synthesised two spinel ferrites were characterized by various techniques. The formation of spinel ferrite nanoparticles was confirmed by Fourier transform infrared (FT-IR) spectroscopy were measured in transmission mode with a Perkin Elmer model-4000 FT-IR infrared spectrometer in the range 400-4000 cm⁻¹. Structure and crystallinity of synthesized nanoparticles was analysed by X-ray diffraction technique (XRD) using GEOL JDX-8P X-ray diffractometer having Cu K α (0.154 nm) radiation to generate diffraction patterns from powder crystalline samples at ambient temperature in a 2 θ range of 20° to 90°. The microstructure and particle size of the nanoparticles were determined from

Scanning electron microscopy (SEM model LEICA S430) images. The crystallinity change during heating was analysed by Differential scanning calorimetry and thermogravimetric analysis (DSC/TGA, model STA 1640) in air at the heating rate of 20oC/min.. The ferromagnetic behavior of synthesized nanoparticles was analysed by using Vibrating sample magnetometer (VSM). The conductivity and dielectric properties was calculated by AC impedance analyser.

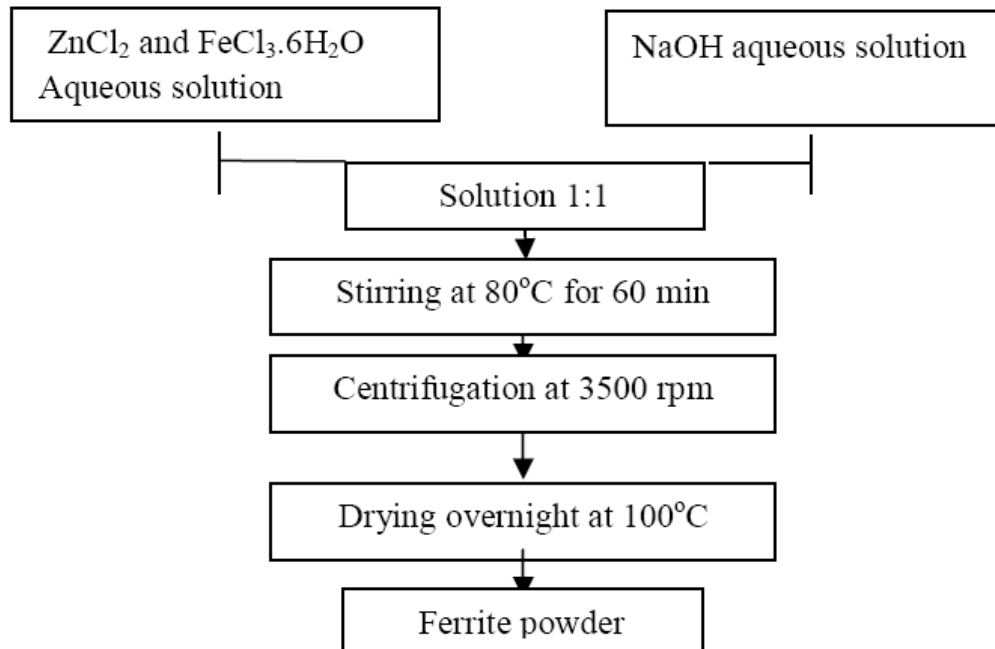


Figure 1: Block diagram to obtain Zinc ferrite nanoparticles

RESULTS AND DISCUSSION

FT-IR analysis

Fig 2 shows the FT-IR spectrum of synthesized Zinc and Barium ferrite nanoparticles. The peaks at 3377 and 3387cm⁻¹ corresponds to stretching vibrations of -OH groups. The peaks at 1614 and 1624cm⁻¹ are caused by flexible vibrations of -OH groups caused by adsorbed water or humidity (Jalaly, M., et al., 2009). It is suggested that the surface of the samples contain active -OH groups. At low wave number, the peaks in the range of 457 to 569cm⁻¹ corresponds to the metal-oxygen (Fe-O) stretching vibrations and it is characteristic peak of the spinel structure of zinc and barium ferrites as reported by Rao, G.S., et al., 1970.

Table 1: FT-IR spectral values of corresponding groups

Vibrational frequencies (cm ⁻¹)	Corresponding groups
3377-3387 cm ⁻¹	Hydroxyl groups
1614-1624 cm ⁻¹	-OH flexible vibrations
457-569 cm ⁻¹	Metal-oxygen bond

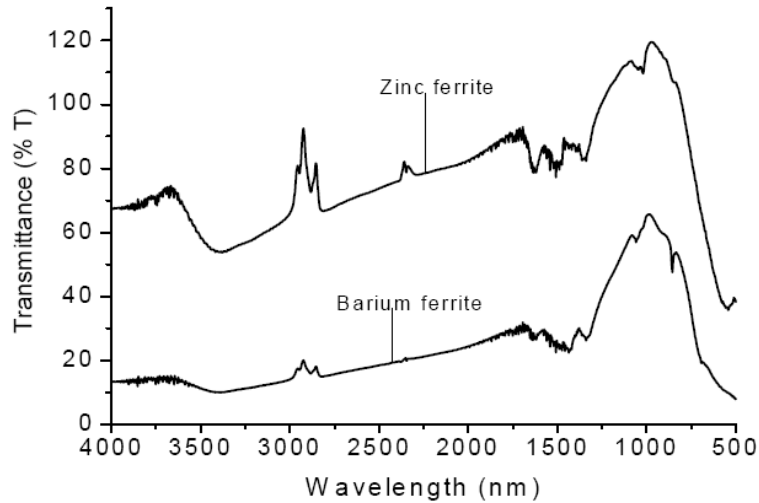


Figure 2: FT-IR spectra of zinc and barium ferrite nanoparticles

XRD analysis

The XRD patterns of the synthesized ferrite nanoparticles are shown in fig 3(a) and (b), which indicates the presence of the spinel cubic structure. The XRD spectra showed all the corresponding to the characteristic planes (220), (311), (511) and (440) of zinc ferrite (Girshick, L., P. Chiu, 1990) and barium ferrite nanoparticles with JCPDS card No. 82-1049 and 46-0113 respectively. Fig 3 shows a typical X-ray diffraction pattern of $ZnFe_2O_4$ and $BaFe_2O_4$ nanoparticles, well-defined diffraction peaks, confirming the formation of nanoparticles. The average crystalline diameter (D) was calculated by Scherrer's equation, $D=0.9\lambda/\beta\cos\theta$

Where, β is the line broadening at the full-width at half maximum (FWHM) of the most intense peak, θ is the Bragg angle and λ is the wavelength of X-rays. The results showed an average crystalline size of zinc and barium ferrite nanoparticles were 82 and 97nm respectively.

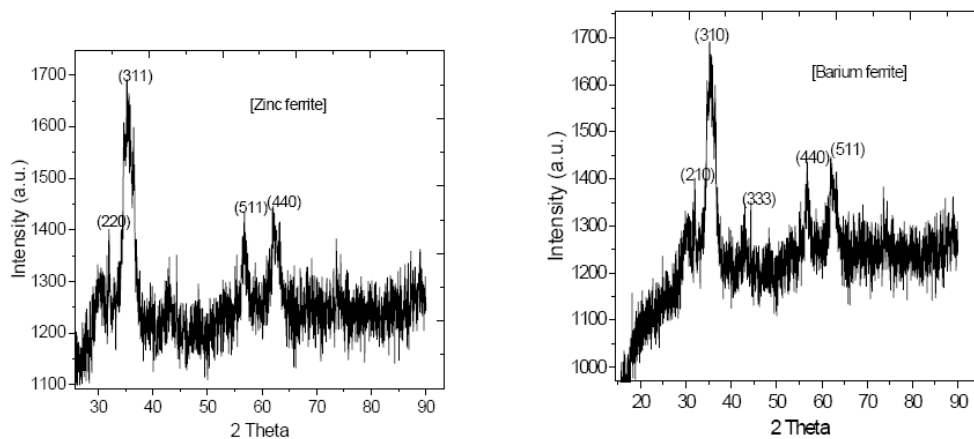


Figure 3 (a) and (b): XRD pattern of Zinc ferrite and Barium ferrite nanoparticles

SEM analysis

It has been observed that the particles are not aggregated, having almost uniform size distribution and the average size of zinc ferrite is 67nm and barium ferrite is 73 nm which are in close agreement with X-ray diffraction data.

DSC analysis

Differential scanning calorimetry is an useful technique for the study of thermal behavior of ferrite nanoparticles. The synthesized ferrite nanoparticles were heated from 100oC to 900oC under flowing N₂ and changes in mass loss are recorded.

VSM analysis

The specific magnetization curves of the investigated samples, obtained from room temperature VSM measurements, are shown in Fig. 4. The magnetization of spinel zinc and barium ferrites originates from the difference in the magnetic moments of the ions at the octahedral lattice sites and those at the tetrahedral lattice sites, and thus directly reflects the distribution of the magnetic Fe³⁺ and non-magnetic Zn²⁺ ions between the two sub lattices. The hysteresis curves are used to check the difference between the soft magnetic materials and the hard magnetic materials. For a hard magnetic material, the area inside the hysteresis loop should be large because it represents the amount of useful magnetic energy that can be made available to do work. But for a soft magnetic material, it represents undesirable core loss .Materials having properties between hard and soft materials are referred to as semi-hard magnetic materials.

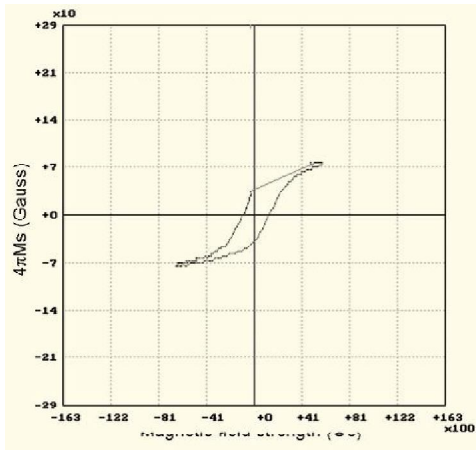


Figure 4(a): Magnetic hysteresis curves measured for Barium ferrite at a room temperature

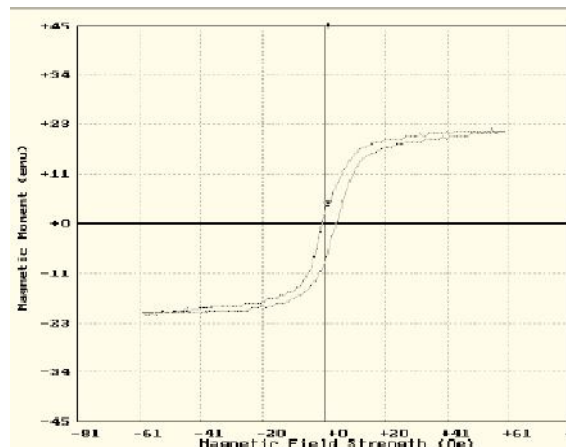


Figure 4(b): Magnetic hysteresis curves measured for Zinc ferrite at a room temperature

AC conductivity

The AC conductivity characteristics of zinc and barium ferrite nanoparticles are shown in fig 5(a) and (b) respectively. The AC conductivity of ferrite samples are measured at room temperature in the frequency range 1 kHz to 1 MHz. The AC conductivity of zinc and barium ferrites increases with increasing frequency gradually and has same values for high frequencies at room temperature. The conductivity values of ferrites, which is due to their semiconducting nature at room temperature and frequencies.

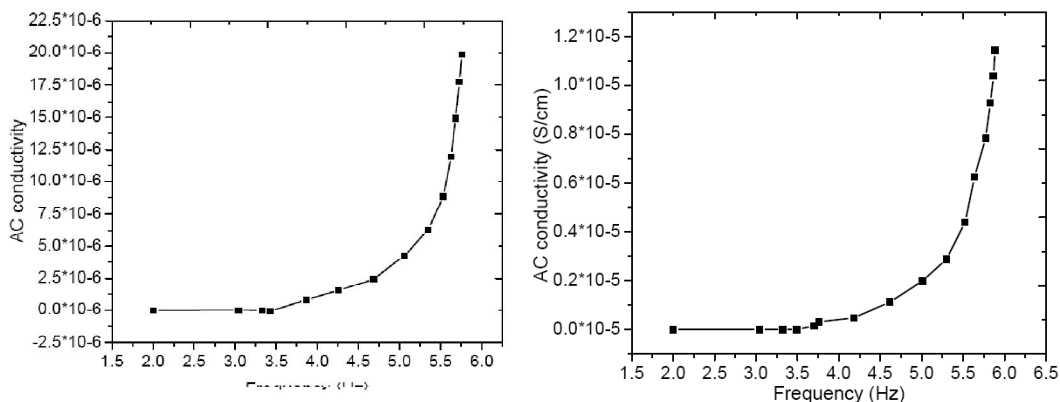


Figure 5(a) and (b): AC conductivity values of Zinc and Barium ferrites

CONCLUSION

Nanosized zinc and barium ferrite particles were synthesized by co-precipitation methods at elevated temperature to analyse the particle size of the compound. The structure of the compound was confirmed by XRD technique. FT-IR analysis supported the formation of spinel structure of ferrite nanoparticles. The FT-IR spectra showed two characteristic metal oxygen vibrational bands, a Fe-O band and Metaloxygen band. Magnetisation measurement has revealed that small particles of zinc and barium ferrites are highly interacting with Fe³⁺ ions on metal surface. The conductivity studies were measured by AC conductivity measurements and the values of zinc and barium ferrite nanoparticles were calculated 19.23×10^{-6} S/cm and 1.13×10^{-5} S/cm respectively makes this ferrite nanoparticles suitable for the high frequency applications. The synthesized nanoparticles are used as potential materials for electrical applications.

REFERENCES

1. Q.A. Pankhurst, J. Connolly, S.K. Jones, J. Dobson., 2003, J. Phys. D Appl. Phys., 36, 167-181.
2. C. Yao, Q. Zeng, G.F. Goya, T. Torres, J. Liu, H. Wu, M. Ge and J.Z. Jiang., 2007, J. Phys. Chem, 111, 12274.
3. E. Torish, G. Shemer and G. Markovich., 2006, Chem mater, 18, 465-470.
4. U. Luders, A. Barthelemy and M. Bibes., 2006, Adv Mater, 18, 1733-1736.
5. Q.A. Pankhurst, J. Connolly and S.K. Jones., 2003, J. Phys D: Appl Phys, 36, 167-181.
6. C.C. Berry., 2005, J. Mater. Chem, 15, 543-547.
7. R.K. Selvan, N. Kalaiselvi, C.O. Augustin Electrochem., 2006, Solid State Commun, 138, 416-421.
8. G.C. Hadjipanayis and R.W. Siegel., 1994, Kluwer Academic Publishers, Dordrecht.
9. S.C. Mojumdar, J. Miklovic, A. Krutoikova, D. Valigura and J.M. Stewart., 2005, J. Therm. Anal Cal, 81, 211.
10. D.H. Kim, D.E. Nikles, D.T. Johnson and C.S. Brazel., 2008, J. Magn. Mater, 320, 2390-2396.
11. J. Wolska, K. Przeoiera, H. Grabowska, A. Przepiera, M. Jablonski and S. Lenert., 2009, Mater. Res. Bull, 44, 15.
12. H. lee, J. Jung, H. Kim, Y. Chung, T. Kim, S. Lee, S. Oh, Y. Kim and I.K. Song., 2008, Catal. Lett, 122, 281.
13. Y. Li, R. Yi, A. Yan, L. Deng, K. Zhou and X. Liu., 2009, Solid State Sci, 11, 1319.
14. C.N. Chinnasamy, A. Narayanasamy and N. Ponpandian., 2000, J. Phy. Cond. Matter, 12, 7795.
15. J. Smit and H. Wjin., 1959, Ferrites Philips Technical Library: Eindhoven .
16. O. Biest and L. Vandeperre., 1999, Annu. Rev. Mater. Sci, 29, 327-352.
17. M. Golosovsky, Y. Saado and D. Davodov., 1999, Appl. Phys. Lett, 7, 4168-4170.
18. M. Atif, S.K. Hasanian and M. Nadeem., 2006, Solid State Commun, 138, 416-421.
19. J.H. Jiang, P. Wynn and S. Morup., 1999, Nanostruct Mater, 12, 737-740.
20. S.D. Shenoy, P.A. Joy and M.R. Anantharaman., 2004, J Magn Magn Mater, 269, 217-226.

21. S. Maensiri, M. Sangmanee and A. Wiengmoon., 2009, Nanoscale Res let, 4, 221-228.
22. S.H. Yu, T. Fujino and M. Yoshimura., 2003, J MagnMagn Mater, 256, 420-427.
23. S. Ammar, N. Jouini, F. Fievet, Z. Beji, L. Smiri, P. Moline and M. Danot., 2006, J. Phys. Condens. Matter, 18, 9055.
24. M. Yang and S.Yen., 2008, Journal of Alloys and Compounds, 450, 387-394.
25. M. Drogenik, M. Kristl, D. Makovec, Z. Jaglicic and D. Hanzel., 2008, Materials and Manufacturing Processes, 23(6), 603-606.
26. A. Bardhan, K. Ghosh, K.Mitra, C.Das, S. Mukarjee and K. Chattopadhyay., 2010, Solid State Sciences, 12, 839-844.
27. M. Swamy, S.Basavaraja, A. Lagashetty, N. Srinivasrao, R.N. Ijagunappa and A. Venkatraman., 2011, Bull. Mater. Sci, 34(7), 1325-1330.
28. G.S. Rao, C.N.R. Rao and J.R. Ferraro., 1970, Appl. Spectrosc, 24, 436. [29] P. Sivakumar, R. Ramesh and A. Ramanand., 2011, Mater Lett, 65, 483-485.



Dr. Urmi Joshi
Government Polytechnic, Jamnagar.